Colloid Polym Sci (2004) 282: 596–601
DOI 10.1007/s00396-003-0984-0

ORIGINAL CONTRIBUTION

C. L. de Vasconcelos
T. N. C. Dantas
M. R. Pereira
J. L. C. Fonseca

Rheology of concentrated alumina-polyelectrolyte systems

Received: 6 June 2003
Accepted: 12 August 2003

C. L. de Vasconcelos · T. N. C. Dantas
M. R. Pereira · J. L. C. Fonseca (✉)
Departmento de Química,
Universidade Federal
do Rio Grande do Norte, Campus
Universitário,
Lagoa Nova, C. P. 1662, RN 59078-970,
Natal, Brazil
E-mail: jlcfonseca@uol.com.br
Tel.: +55 0 84 215 3828
Fax: +55 0 84 211 9224

Abstract Rheological properties of concentrated alumina suspensions using a charged copolymer as the dispersant have been studied. The non-Newtonian behavior of these fluids was characterized and correlated to ζ potential measurements and sedimentation column data, obtained with these dispersions. As a result, a clear relationship between dispersion stability and pseudoplastic/dilatant rheological behavior was established.

Keywords Alumina suspensions · Rheology · Flocculation · Polyelectrolyte

Introduction

Colloidal suspensions are used in several industrial applications such as paper making [1], ceramic processing [2], paints [3], detergents [4], cosmetics [5], food concentrates [6], and pharmaceutical products [7, 8]. In these applications many of these systems need hydrodynamic stabilization so that suitable properties, such as adequate shelf life, may be obtained. The most effective mechanism of stabilization of these colloidal systems against particle irreversible aggregation results from inter-particle repulsive forces, arising from the adsorption of suitable chemical species onto the particle surfaces [9]. When working with aqueous systems, the use of polyelectrolytes as stabilization agents has played an important role [10], mainly because it involves, regarding particle-particle interactions, repulsive electrostatic forces, which yield electrosteric repulsion, preventing irreversible colloidal particle aggregation [11, 12]. Conversely, in order to obtain particular processability properties, polyelectrolytes may be used as agents for the destabilization of colloidal dispersions, through the use of forces originating from the formation of inter-particular bridging, resulting in the flocculation of aqueous dispersions [13]. In previous works, our group has characterized the occurrence of these inter-particle forces, which were involved in the destabilization of alumina dispersions by bridging flocculation [14, 15].

These inter-particle forces and colloidal interactions in concentrated colloidal suspensions have motivated the description of their influence on the rheological properties of colloids [16]. Rheological behavior of colloidal systems has been investigated, from negatively charged and hydrated particles [17] to hydrophobic ones [18], in order to analyze the non-Newtonian effects. Non-Newtonian behavior occurs in flocculated colloidal suspensions because of interactions between the dispersed particles and macromolecules, as well as inter-particle forces, resulting in a contribution to the structural arrangement of the particles in the applied flow field, and hence the rheological behavior of the suspension [19]. These inter-particle forces are attributed to London-van der Waals attraction, electrostatic repulsion, and forces related to polymer adsorption, which determine the dispersion stability.

In the specific case of alumina, the interactions of charged copolymers with solids and their effect on the behavior of suspensions with high contents of solid have already been studied [20]. The purpose of the present work is to propose a connection between rheology, polyelectrolyte solution properties, and inter-particle forces for concentrated alumina dispersions, using rheometry, ζ potential measurements, and settling experiments.

Experimental

Materials

The alumina powder (Alcoa Alumïnio, Brazil) used in this work was comprised of particles with average diameter of (2.1–3.1) μm, according to the supplier. The average surface area, as measured by standard BET N_2 adsorption, was (1.4–1.7) $m^2\ g^{-1}$; the chemical analysis data, expressed in terms of weight percentage, were: Al_2O_3 (99.4–99.7)%, SiO_2 (0.03–0.05)%, Fe_2O_3 (0.038–0.050)% and Na_2O (0.11–0.14)%. The polyelectrolyte used in this work was a sodium salt of poly(styrenesulfonic acid-*co*-maleic acid) ($M_w \approx 2.0\times10^4$ g mole^{-1}, Fig. 1, Aldrich, USA, used as received), with a molar ratio 1:1 for styrene to maleic acid. NaCl (P.A., Vetec, Brazil) was used as received.

Preparation of suspensions

Alumina suspensions were prepared with 20.0 wt% of solids, for rheological measurements and settling experiments, and 1.50 wt% for zeta potential measurements. The experiments were performed at two salt concentrations: [NaCl] = 3.00×10^{-3} mole L^{-1} (system which was defined as being of low ionic strength) and [NaCl] = 3.00×10^{-2}mole L^{-1} (high ionic strength system), both systems with polymer concentrations of 20.0 g L^{-1}, 1.00 g L^{-1}, 0.250 g L^{-1}, and 2.50×10^{-4} g L^{-1}. All the suspensions were made with bi-distilled water, immersed in an ultrasonic bath (Transsonic model T460, Germany) for 1 min. In the case of ζ potential measurements and settling experiments, it was experimentally found that an adsorption time of 4 days was necessary to reach equilibrium (constant results). In the case of rheometry, this time was found to be 24 h.

Electrophoretic measurements

Electrophoretic mobilities of the alumina dispersions were determined with a particle concentration of 0.500 g L^{-1}. This concentration was achieved by the dilution of dispersions with a solid content of 1.50 wt% , using copolymer solutions with the same concentration in the disperser phase, before measurements were carried out. The electrophoretic mobility measurements, μ_E, were carried out using a Zeta-Meter System 3.0+ (Zeta-Meter, USA). The ζ potential values for alumina dispersions were calculated from μ_E by employing the Smoluchowski relationship [21]:

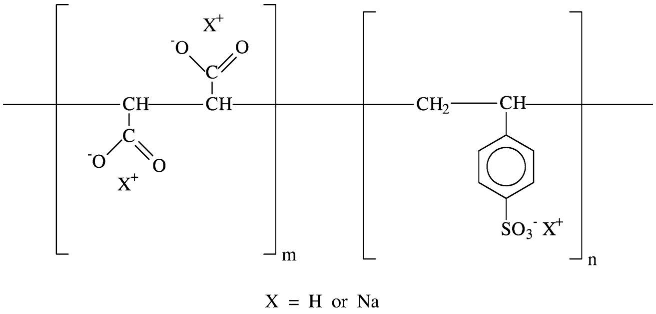

Fig. 1 Chemical structure of the polyelectrolyte used in this work

$$\zeta = \frac{\mu_E \eta}{\epsilon_0 \epsilon}, \qquad (1)$$

where ϵ_0 is the permittivity of vacuum, ϵ is the dielectric constant of water, and η is the viscosity of the medium.

Rheological measurements

Alumina suspensions used in these experiments were obtained as described. All the experiments were conducted at a temperature of 30.0 ± 0.1 °C. The measurements were carried out in a cone-plate type Brookfield rheometer, USA, model LDV-III, using spindle CP40 and consisted of collecting data relating apparent viscosity, η, to shear rate, $\dot{\gamma}$. According to the manufacturer's instructions, experimental errors involved in the determination of torque were 1% of its full scale, regardless of the torque magnitude. All experiments which were considered valid were in a range of torque from 10% of its full scale (implying a maximum relative experimental error of 10%) to 90% (which was indicated by the manufacturer as the point at which the behavior of their elements as a Hookean spring was not reliable).

Settling experiments

Alumina suspensions were transferred (volume 110 mL) to a column of 24 cm height and 3 cm diameter. The suspensions were allowed to reach equilibrium for 30 days, in order to obtain the sedimentation volume of the particles.

Results and discussion

Figure 2 shows a plot of $\dot{\gamma}$ for the polyelectrolyte solutions (without alumina particles) at high and low ionic strength media, at different polyelectrolyte concentrations. One can observe that, within the experimental error and range of shear rate, the solutions behave as Newtonian fluids. It can also be noted that, for a given polymer concentration, lower ionic strength solutions yielded higher viscosity values. This behavior has been widely reported for polyelectrolytes [22]: when increasing polyelectrolyte or counterion concentration, there is the occurrence of electrical shielding between macromolecular charges. As a consequence, repulsion between these charges decreases, as well as macromolecular dimensions, resulting in a decrease of solution viscosity, which is a macroscopic response largely influenced by these dimensions.

In Fig. 3, η is represented as a function of $\dot{\gamma}$, for alumina suspensions with polyelectrolyte concentrations of 20.0 g L^{-1} and 1.00 g L^{-1} at high and low ionic strengths. One can see that there is no evident difference between the profiles presented for systems with the same

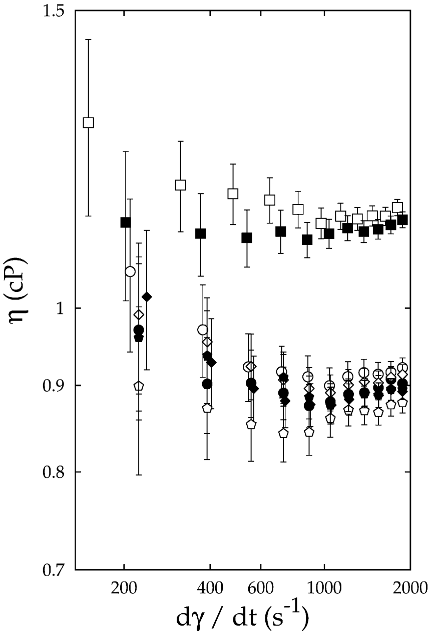

Fig. 2 Plot of η as a function of $\dot{\gamma}$ for the polyelectrolyte solutions: 20.0 g L^{-1} (*squares*), 1.00 g L^{-1} (*circles*), 0.250 g L^{-1} (*diamonds*), 2.50×10^{-4} g L^{-1} (*pentagons*). *Open circles* [NaCl] = 3.00×10^{-3} mol L^{-1}. *Filled circles* [NaCl] = 3.00×10^{-2} mol L^{-1}

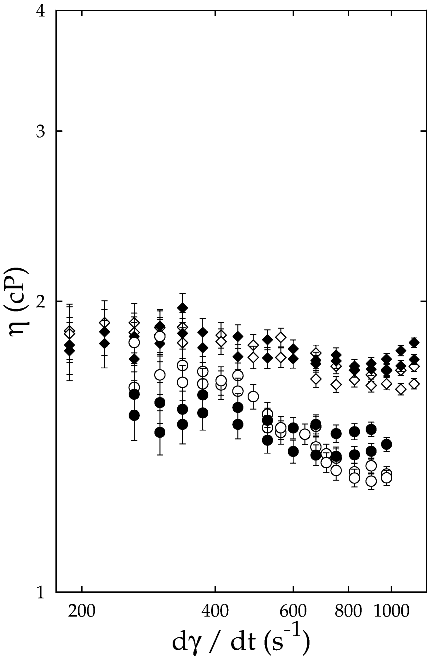

Fig. 3 Plot of η as a function of shear rate, $\dot{\gamma} = d\gamma/dt$, for the alumina suspensions. Polyelectrolyte concentrations: 20.0 g L^{-1} (*diamonds*), 1.00 g L^{-1} (*circles*). *Open symbols* [NaCl] = 3.00×10^{-3} mole L^{-1}. *Filled symbols* [NaCl] = 3.00×10^{-2} mole L^{-1}

polymer concentrations at different ionic strengths. The dispersions are initially characterized by a tendency to pseudoplastic behavior, which was more pronounced at the polyelectrolyte concentration of 1.00 g L^{-1}. As shear rate is increased, one can observe a range in which viscosity is constant up to a critical shear rate, which is dependent on polyelectrolyte concentration. Further increase in shear rate results in the dispersion behavior as dilatant fluids. The destruction of particle aggregates, as a result of shear, commonly occurs in highly concentrated dispersions, since colloidal and hydrodynamic interactions may result in the formation of these aggregates [23]. Particle aggregation may be followed by destruction of these very aggregates, resulting in a perturbation of suspension structure in the flow field and, consequently, in pseudoplastic behavior [24]. From this point, a narrow shear rate range with constant viscosity can be observed, followed by an increase in viscosity, which is due to particle orientation by the flow of the disperser phase: this orientation favors inter-particle interactions, resulting in new clustering, as already been characterized by Bender et al. in some particulate systems [25]. Other authors have attributed the shear thickening to an order–disorder transition of the colloidal structure [26]. These authors found that flow lines would be destroyed in the less ordered state at a critical shear rate. In this less ordered state there would be the occurrence of interpenetration of flow lines, which would lead to the occurrence of turbulent flow and, as a consequence, the increase in energy dissipated per volume unit of sheared dispersion, $\dot{w}$, resulting in an increase in apparent viscosity [27], as shown by:

$$\dot{w} = \eta\dot{\gamma}^2 \tag{2}$$

Figure 4 shows a plot of $\eta \times \dot{\gamma}$ for alumina dispersions with polyelectrolyte concentrations of 0.250 and 2.50×10^{-4} g L^{-1}, at different ionic strengths. One can observe, again, that within the experimental errors, there is no pronounced difference for systems which only differ in ionic strength. The suspensions with a polyelectrolyte concentration of 2.50×10^{-4} g L^{-1}, however, present a more accentuated pseudoplastic behavior than all the other dispersions. It can be related to the mentioned results already obtained by our group [14, 15]. Through experiments on the kinetics of settling of these dispersions and viscometry of the disperser phase, it was possible to characterize that the mechanism involved in their flocculation was based on polymer bridging. This sort of flocculation occurs when polymer chains simultaneously adsorb on the surfaces of different particles. Polymer bridging represents long range forces and occurs in systems with a low surface coverage by the adsorbed polymer [28]. As a consequence, viscosity measurements at different polyelectrolyte concentrations in the present work suggest that the shear-thinning may

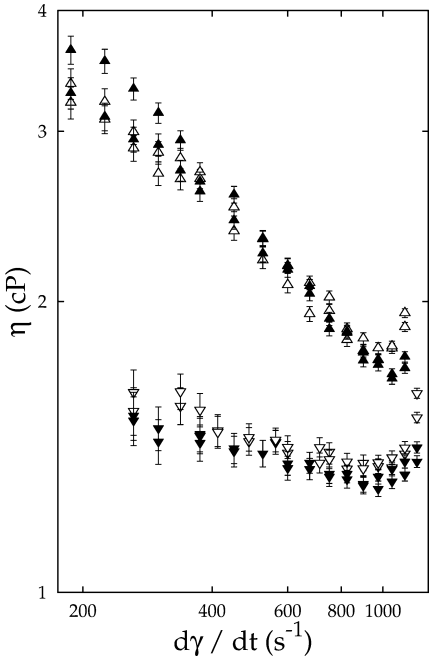

Fig. 4 Plot of η as a function of shear rate, $\dot{\gamma} = d\gamma/dt$, for alumina suspensions with polyelectrolyte concentrations of 2.50×10^{-4} g L^{-1} *(up triangles)*, and 0.250 g L^{-1} *(down triangles)*. *Open symbols* [NaCl] = 3.00×10^{-3} mol L^{-1}. *Filled symbols* [NaCl] = 3.00×10^{-2} mol L^{-1}

Table 1 Zeta potential values for the alumina dispersions with the different polymer concentrations and NaCl molarities used in this work

C	ζ	
(g L^{-1})	[NaCl] = 3.00×10^{-3} M (mV)	[NaCl] = 3.00×10^{-2} M
0	57 ± 1	41.3 ± 0.9
2.50×10^{-4}	−15 ± 1	−34 ± 2
0.250	−60 ± 2	−57 ± 2
1.00	−78 ± 2	−61 ± 2
20.0	−59 ± 2	−60 ± 3

ζ Zeta potential, *C* polymer concentration, [NaCl] NaCl molarity

be related to the macromolecular dimensions. As at lower polyelectrolyte concentrations the polyelectrolyte chains are more extended, it may result in bigger macromolecular clusters (as a result of hydrogen bonds and electrostatic interactions between the positive-charged sites on the particle surface and anionic sites on the polyelectrolyte chain) which can be reduced in size by shearing. Therefore, one can suggest that the shear-thinning of concentrated alumina suspensions flocculated by polymer bridging is a result of breaking of physical network structures. Alumina suspensions without polyelectrolyte presented rather random fluctuations in viscosity for all shear rates, a result which strengthens the evidence of the polyelectrolyte role in the structure formation in these dispersions.

Table 1 shows the values of ζ potential for the samples used in this work. In the case of pure alumina dispersions, ζ potential has a lower value for the high ionic strength dispersion. Since, in this case, one has no polyelectrolyte molecules in the disperser medium, these differences should be analyzed in terms of purely electrostatic interactions, involving low molecular weight ions. As ionic strength increases, double layer thickness decreases, the modulus of ζ decreasing as a consequence [29]. Regarding disperser media with solubilized polyelectrolyte, one can see that all ζ potential values reflect the adsorption of these negatively charged macromolecules on the alumina surface. For a polymer concentration of 2.50×10^{-4} g L^{-1}, ζ potential values are markedly different, the values for higher ionic strength being much more negative than the ones for low ionic strength. It can be explained as a consequence of a more pronounced polyelectrolyte effect in the case of the high ionic strength dispersions: the macromolecular chains are less extended in solution, as a result, more macromolecules would be adsorbed *per* particle, resulting in more negative ζ potential values. At the next polymer concentration, 0.250 g L^{-1}, ζ potential values are the same, within the experimental errors, for both ionic strengths. It indicates that as polymer concentration increases, due to the higher presence of polyelectrolyte counterions, the polyelectrolyte effect begins to minimize. However, for the polymer concentration of 1.00 g L^{-1}, we observe the inverse situation to that observed at 0.250 g L^{-1}: the dispersion at lower ionic strength has the most negative ζ potential. It can be explained as the result of a drastic decrease in macromolecular dimensions as polymer concentration increases. This decrease would be more pronounced in the case of the lower ionic strength dispersion, due to poorer low molecular weight electrolyte shielding; in the same way, as low molecular weight electrolyte concentration is higher, polyelectrolyte counterions would be more condensed, resulting in less negative ζ potential values. For the polymer concentration of 20.0 g L^{-1}, again, ζ potential values do not differ for high and low ionic strengths. In this case, polymer concentration is so high that low molecular weight electrolyte concentration does not make any difference, in terms of macromolecular dimensions and polyelectrolyte counterion condensation.

Table 2 shows the volumetric fractions of settled particles, ϕ, as a function of polyelectrolyte concentration and ionic strength. One can see that there is a tendency of a higher ϕ for the high ionic strength dispersions, mainly at a concentration of 0.250 g L^{-1}: in this case the sediment of the low ionic strength dispersion surely is more compacted than the high ionic strength one. Adsorbed polyelectrolyte may influence ϕ in two opposite ways: (1) increasing ϕ, through electrosteric interactions and (2) decreasing ϕ through the formation of more compacted sediments, resultant

Table 2 Volumetric fraction of the sedimented particles in the column of sedimentation for the alumina suspensions at the different polyelectrolyte concentrations and NaCl molarities

C	ϕ	
(g L^{-1})	[NaCl] = $3.00{\times}10^{-3}$ M	[NaCl] = $3.00{\times}10^{-2}$ M
0	0.174 ± 0.006	0.181 ± 0.006
$2.50{\times}10^{-4}$	0.185 ± 0.006	0.190 ± 0.006
0.250	0.110 ± 0.006	0.128 ± 0.006
1.00	0.107 ± 0.006	0.112 ± 0.006
20.0	0.115 ± 0.006	0.121 ± 0.006

ϕ Volumetric fraction, C polyelectrolyte concentration, [NaCl] NaCl molarity

from inter-particle bridging, as discussed before. When concentration varies from 0 to $2.50{\times}10^{-4}$ g L^{-1}, it seems that the first process is dominant; further increase in polyelectrolyte concentration results in the rule of the second one: some physical crosslinking must have occurred in order to compact the sedimentation volume of the suspensions of alumina with higher concentration of polyelectrolyte. Somasundaran et al. [30] have demonstrated that charged groups in anionic polymer chains may form complexes with hydrolyzed charged species positively charged, such as Al^{3+}, $Al(OH)_2{}^{+}$, and $AlOH^{2+}$, present in the dispersion. Indeed, it was found in the disperser phase of these suspensions, using atomic absorption spectroscopy, Al^{3+} cations, at a concentration of (12 ± 2) mg L^{-1} [15]. It suggests that the agents involved in this physical crosslinking would be on the alumina surface, but also within the disperser phase. In other words, the increase in the state of compacting of the particles would have a component coming from the electrostatic interactions between Al^{3+} ions, present in the alumina suspensions and anionic groups present in the polyelectrolyte chains. The same sort of physical crosslinking may be found in the case of the interaction between polycharged ions and anionic polysaccharide molecules, in the process of polymer gelling [31, 32].

Conclusion

Rheology of aqueous alumina–polyelectrolyte systems is closely bound to their stabilities. The pseudoplastic behavior of these dispersions is a consequence of the destruction of structures such as the ones provenient from the formation of particle clusters from bridging flocculation; posterior shear-thickening was due to the orientation of these particles and/or turbulent flow. Polymer bridging also influenced sedimentation volumes in two ways: increasing it, as a consequence of electrosteric interactions (which are related to ζ potential values), and decreasing it, as a consequence of sediment compacting by polyelectrolyte–alumina ionic crosslinking.

Acknowledgments The authors thank Brazil's Ministério da Ciência e Tecnologia (MCT), Conselho Nacional de Desenvolvimento Científico e Tecnológico (CNPq), Fundação Coordenação de Aperfeiçoamento de Pessoal de Nível Superior (CAPES), Banco do Nordeste, and Pró-Reitoria de Pesquisa e Pós-Graduação da Universidade Federal do Rio Grande do Norte (PPPg-UFRN) for financial support during the course of this work.

References

1. Gomoiu I, Catley BJ (1996) Enzyme Microb Tech 19:45
2. Davies J, Binner JGP (2000) J Eur Ceram Soc 20:1569
3. Croll S (2002) Prog Org Coat 44:131
4. Walde P, Ichikawa S (2001) Biomol Eng 18:143
5. Colic M, Fuerstenau DW (1998) Powder Technol 97:129
6. Dickinson E (2003) Food Hydrocolloid 17:25
7. Levis SR, Deasy PB (2002) Int J Pharm 243:125
8. Silvander M, Hellstrom A, Warnheim T, Claesson P (2003) Int J Pharm 252:123
9. Boisvert JP, Persello J, Castaing JC, Cabane B (2001) Colloids Surf A Physicochem Eng Aspects 178:187
10. Boris DC, Colby RH (1998) Macromolecules 31:5746
11. Pettersson A, Marino G, Pursiheimo A, Rosenholm JB (2000) J Colloid Interface Sci 228:73
12. Romero-Cano MS, Martïn-Rodrïguez A, Chauveteau G, de las Nieves FJ (1998) J Colloid Interface Sci 198:273
13. Kiratzis N, Faers M, Luckham PF (1999) Colloids Surf A Physicochem Eng Aspects 151:461
14. de Vasconcelos CL, de Medeiros DWO, de Moura KT, Acchar W, Dantas TNC, Pereira MR, Fonseca JLC (2003) Powder Technol 133:164
15. de Vasconcelos CL, de Moura KT, de Medeiros DWO, Moura KT, Morais WA, Dantas TNC, Pereira MR, Fonseca JLC (2003) Powder Technol (submitted)
16. Zhou ZW, Scales PJ, Boger DV (2001) Chem Eng Sci 56:2901
17. Poncet-Legrand C, Lafuma F, Audebert R (1999) Colloids Surf A Physicochem Eng Aspects 152:251
18. Berli CLA, Deiber JA, Añón (1999) Food Hydrocolloid 13:507
19. Baklouti S, Romdhane MRB, Boufi S, Pagnoux C, Chartier T, Baumard JF (2003) J Eur Ceram Soc 23:905
20. Kamiya H, Fukuda Y, Suzuki Y, Tsukada M, Kakui T, Naito M (1999) J Am Ceram Soc 82:3407
21. Hunter RJ (2001) Colloids Surf A Physicochem Eng Aspects 195:205
22. Fernandes ALP, Martins RR, da Trindade Neto CG, Pereira MR, Fonseca JLC (2003) J Appl Polym Sci 89:191

23. Starov V, Zhdanov V, Meireles M, Molle C (2002) Adv Colloid Interface Sci 96:279
24. Bergström L (1998) Colloids Surf A Physicochem Eng Aspects 133:151
25. Bender J, Wagner N (1996) J Rheol 40:899
26. Catherall AA, Melrose JR, Ball RC (2000) J Rheol 44:1
27. de Vasconcelos CL, Pereira MR, Fonseca JLC (2001) J Appl Polym Sci 80:1285
28. Biggs S (1995) Langmuir 11:156
29. Melis S, Kemmerer M, Meuldijk J, Storti G, Morbidelli M (2000) Chem Eng Sci 55:3101
30. Kalyan DD, Somasundaran P (2001) Colloids Surf A Physicochem Eng Aspects 182:25
31. Rodd AB, Cooper-White JJ, Dunstan DE, Boger DV (2001) Polymer 42:3923
32. Miyazaki Y (1995) Polyhedron 14:1961